

Narrowly Size Distributed Zinc-Containing Poly(acrylamide) Latexes via Inverse Miniemulsion Polymerization

Elena Kobitskaya,[†] Duygu Ekinici,[†] Achim Manzke,[‡] Alfred Plettl,[‡] Ulf Wiedwald,[‡] Paul Ziemann,[‡] Johannes Biskupek,[§] Ute Kaiser,[§] Ulrich Ziener,^{*,†} and Katharina Landfester^{*,†,⊥}

[†]*Institute of Organic Chemistry III, Macromolecular Chemistry and Organic Materials, University of Ulm, Albert-Einstein-Allee 11, 89081 Ulm, Germany,* [‡]*Institute of Solid State Physics, University of Ulm, Albert-Einstein-Allee 11, 89081 Ulm, Germany,* [§]*Transmission Electron Microscopy Group, University of Ulm, Albert-Einstein-Allee 11, 89081 Ulm, Germany,* and [⊥]*Max Planck Institute for Polymer Research, Ackermannweg 10, 55128 Mainz, Germany*

Received November 19, 2009; Revised Manuscript Received February 10, 2010

ABSTRACT: Polyacrylamide nanoparticles containing zinc nitrate were prepared via inverse miniemulsion polymerization using ultrasound emulsification. The effects of sonication time, mode of sonication, nature and type of emulsifier, amount of zinc salt, solvent in the dispersed phase, nature of dispersed and continuous phases, and type of initiator on the nucleation mechanism, conversion, molecular mass of polymer, and size distribution of the latex particles were investigated. The results showed that an increase in sonication time up to 4 min and using an amphiphilic polymeric surfactant with a relatively short hydrophilic part improved both the monodispersity and the stability of the zinc-containing latexes. An increase in viscosity of the continuous phase (changed by means of different nonpolar solvents) and decrease in viscosity of the dispersed phase (varied by the amount of water) had also a positive effect on the monodispersity. At the same time, the average diameter of the particles in the range of 225 nm changed only marginally. The use of either highly hydrophilic (ammonium persulfate) or highly hydrophobic (2,2'-azobis(2-methylbutyronitrile)) initiators, and the transfer from miniemulsion polymerization to dispersion, precipitation, or a combination of several polymerization types by the modification of the dispersed and continuous medium spread the polydispersity of the latex particles and impaired the stability. Samples with small content of salt were used for unconventional nanolithography by subjecting a highly ordered layer of the nanoparticles to a plasma etching process. Highly ordered arrays of particles containing ZnO nanocrystals were observed.

Introduction

In recent years more and more attention has been paid to the synthesis and properties of metal and metal oxide nanoparticles. Because of the small size those objects exhibit unique physico-chemical properties. For example, nanometer-sized zinc oxide (ZnO) is a semiconductor with an optical bandgap in the UV region. However, the main problem in the utilization of nanoparticles is their poor long-term size stability in solution because of their tendency to aggregate due to the high surface area-to-volume ratio. Usually, this problem is solved by surface modification of the nanoparticles. As coatings inorganic substances (e.g., homogeneously Al₂O₃-coated ZnO nanoparticles¹) as well as organic surfactants² and polymers (as micellar stabilizer³ or as matrix for ZnO nanoparticles^{4–6}) can be employed. There are still certain drawbacks, in particular with the deposition of the nanoparticles on the substrate, what is highly intriguing for a regular functionalization of a surface as well as for further manipulation of the particulate arrays, e.g., growing of nanopillars.⁷

Despite of the possibility to form highly organized metallic nanoparticle arrays, the micellar technique comprises some restriction with respect to the interparticle distance and the metal content.⁸ In the case of composite materials the situation is more

complicated. Bulk polymerization of a ZnO particle–monomer mixture results in the segregation of primary particles with the formation of domains with different sizes, which are more or less homogeneously distributed in the polymer matrix.⁵ A more effective method to obtain polymer/inorganic composite particles is the miniemulsion polymerization based on the nanoreactor concept.⁹ By this approach, nanosized magnetic iron oxide was successfully encapsulated either in a polystyrene matrix^{10,11} by direct miniemulsion polymerization or a polyacrylamide (PAAm) matrix¹² by inverse miniemulsion polymerization. Partially neutralized acrylic acid was polymerized in the presence of ZnO nanoparticles in the continuous phase of a miniemulsion forming poly(acrylic acid-*co*-sodium acrylate)/zinc oxide composite latex particles.⁶ The best results with respect to the monodispersity of nanoparticles and the formation of highly ordered metallic nanoparticle arrays on a silicon substrate were obtained by a two-step technique.^{13,14} Here, precursor complexes of different metals were encapsulated in polystyrene nanoparticles via direct miniemulsion polymerization in the first step. In the second step the hybrid particles were deposited by self-assembly onto a silicon substrate in hexagonally ordered arrays and were subjected to a plasma etching and annealing process. As a result the polymer was removed leaving behind metal particles, the ordering of which maintained the assembly of the original composite particles. The distance between the metal particles was regulated by controlling the size of the initial latex particles. A severe restriction of this general concept is the limitation of

*To whom correspondence should be addressed. (K.L.) E-mail: landfester@mpip-mainz.mpg.de. Telephone: +49 6131 379170. Fax: +49 6131 379170. (U.Z.) E-mail: ulrich.ziener@uni-ulm.de. Telephone: +49 731 5022884. Fax: +49 731 5022883.

solubility of metal salts in the nonpolar medium, in this case the monomer. The transfer to inverse miniemulsion polymerization, where the dispersed phase is a polar (water-soluble) monomer, can greatly enhance the variety of applicable metal salts as well as the encapsulated amount of the inorganic compound. Typical hydrophilic monomers like hydroxyethyl methacrylate, acrylamide, or acrylic acid were successfully polymerized in inverse miniemulsion.^{15–18} Contrary to the direct systems (ultra)lipophobic osmotic pressure agents have to be employed.⁹ Such lipophobic compounds are often salts, e.g., sodium chloride,^{15,18} magnesium sulfate,¹⁷ copper bromide, and copper chloride.¹⁶ In inverse heterophase systems, relatively narrow latex particle size distributions could also be achieved.¹⁵

Here, we report on the synthesis of narrowly size distributed PAAm–Zn(NO₃)₂ particles by an inverse miniemulsion process. Various factors like time and type of sonication, nature of the solvent, concentration of the metal salt, type of emulsifier, etc. influence the latex particles' size and size distribution. In general, these parameters can be divided into two groups: (i) the parameters affecting the preparation of the initial emulsion; (ii) the parameters affecting the behavior of the system during polymerization. Since some factors (for example, nature of the polar solvent) can influence not only the miniemulsification process but also the polymerization, it is important to keep control over both the colloidal properties of the latexes and the characteristics of the resulting polymers. In the final part of the present paper we have shown the applicability of the composite particles for the preparation of two-dimensional arrays of ZnO-containing nanoparticles by plasma etching.

Experimental Part

Reagents and Materials. Acrylamide (AAm, Aldrich) was recrystallized twice from chloroform and then vacuum-dried. Zinc(II) nitrate hexahydrate (99%, Fluka), Isopar M (a C12–C14 isoparaffinic mixture, Caldico Deutschland Chemie B.V.), 2,2'-azobis(2-methylbutyronitrile) (V59, Wako), and sorbitan monostearate (Span 60, Aldrich) were used as received. Polymeric surfactants poly(ethylene-co-butylene)-*block*-poly(ethylene oxide) with different molecular weights (P(E/B)-PEO-6 with $M_n = 5800 \text{ g}\cdot\text{mol}^{-1}$, 31 wt % of ethylene oxide (EO), HLB = 6.2; P(E/B)-PEO-7 with $M_n = 7400 \text{ g}\cdot\text{mol}^{-1}$, 46 wt % of EO, and HLB = 9.2; P(E/B)-PEO-10 with $M_n = 9750 \text{ g}\cdot\text{mol}^{-1}$, 59 wt % of EO, HLB = 11.8, see Supporting Information) were synthesized by anionic polymerization as described elsewhere.¹⁹ 2,2'-Azobis(isobutyronitrile) (AIBN, Aldrich) was recrystallized from methanol and vacuum-dried. Ammonium persulfate (APS, Aldrich), toluene, ethanol, cyclohexane (CH), tetrahydrofuran (THF), dimethyl sulfoxide (DMSO), acetonitrile (AN), acetone, isooctane, and *n*-hexadecane (HD) were of analytical grade and used as received from Merck. Syntheses and analyses were performed with demineralized water of Milli-Q grade (resistivity: 18 M Ω).

Synthetic Methods. The aqueous phase was prepared as follows. The zinc salt was dissolved in a polar solvent (water, ethanol, THF, acetone, AN, or DMSO) in the respective ratio. The polar phase will be denoted further as "aqueous phase". Then AAm (1 g, 1.4×10^{-2} mol) was added to the salt solution. In the case of low water content, this mixture was carefully heated until complete dissolution of AAm. The oil phase was prepared by dissolution of a suitable amount of emulsifier in a nonpolar solvent (isooctane, CH, isopar M, or HD) at 60 °C. In all syntheses the amount of emulsifier was kept at 2 wt % with respect to the aqueous phase and the weight ratio of W/O was 1/4. Then both the aqueous and the oil phase were transferred to a screw cap vessel and miniemulsified by ultrasonication with a sonifier (W450 Digital,

Branson, Danbury, CT) at 90% amplitude (tip $1/2$ in.) for 240 s. To avoid premature polymerization, the mixtures were cooled with an ice-bath during sonication. The polymerization reactions were carried out in a three-necked flask (50 or 100 mL) equipped with a reflux condenser, argon inlet, and magnetic stirrer. Before polymerization, the miniemulsion was purged with argon for 30 min. To initiate the polymerization, the temperature was raised to 65 °C, and a solution of AIBN (7×10^{-5} mol) in toluene (0.30 mL) was added. To ensure full conversion of the monomer, the reaction mixture was stirred at 65 °C for 4 h in the case of water as aqueous phase and for 24 h for other solvents.

In the case of polymerization with the hydrophilic initiator APS the following procedure was performed. A solution of APS (7×10^{-5} mol) in water (0.1 g) was added to the solution of the salt and AAm in water. Then both phases were rapidly transferred to a screw cap vessel and miniemulsified by ultrasonication as described above. The reaction mixture was stirred at 60 °C for 24 h.

Table 1 shows the amounts of the employed components, the reaction conditions, and the characteristics of the resulting latexes.

Analytical Methods. The size of the particles and the droplets (*Z*-average hydrodynamic diameter, D_h) and size distribution (polydispersity index, PDI) were measured by dynamic light scattering (DLS, Malvern Zetasizer Nano-series) at 20 °C under the scattering angle of 173°. A helium/neon laser operating at 633 nm with 4.0 mW was used as a light source.

Basic transmission electron microscopy (TEM) was performed with a Philips EM400 electron microscope operating at 80 kV. High resolution (HR) TEM was performed with a FEI Titan 80–300 (300 kV operating voltage) using an imaging side aberration corrector (CEOS type). A point-to-point resolution of better than 0.1 nm in HRTEM was given after minimizing of aberration up to the third order (resulting phase plate 20 mrad). Scanning (S) TEM was performed on the same FEI Titan 80–30 system using a Fischione high angle annular dark-field (HAADF) detector and nominal STEM probe size of smaller than 0.14 nm.

The polymer suspension after synthesis was diluted with the appropriate nonpolar solvent and then dropped onto a 400 mesh carbon-coated copper grid and left to dry. Free-standing ultrathin membranes of SiN (30 nm thick, SPI Company) were used as substrate to study plasma etched ZnO particles (see details of plasma processing later in the text) by TEM.

Further analyses were done on a Hitachi S-5200 high-resolution scanning electron microscope (HRSEM). The acceleration voltage as well as the extraction current was kept constant for all samples at 30 kV and 10 μ A, respectively.

The viscosity of the aqueous and continuous media was measured using a Haake MARS RheoStress 6000 rheometer in a thermostatically controlled measuring unit "plate/plate" (PP60/Ti). The temperature was 23 °C. Shear rates were varied in the range from 80 to 150 s^{-1} . In this region of shear rates no deviation from Newtonian flow was observed and the viscosity values were constant (Table 2).

The conversion of monomer was determined by gravimetry. After miniemulsion polymerization about 1 mL of the latex was dropped into excess acetone, the precipitate was filtered, and the residue was dried at 75 °C to constant weight.

The thermal behavior of seven samples with different amounts of salt (samples 11, 12, 13, 14, 15, 16, and 17; see Table 1) has been investigated by differential scanning calorimetry (DSC) on a Perkin-Elmer DSC-7 differential

Table 1. Recipes and Characteristics of the Resulting Latexes

no.	dispersed phase		continuous phase		D_h (nm) ^a	PDI ^b	yield (%)
	salt (g)	solvent, amt (g)	solvent	emulsifier, amt (wt %)			
Initiator AIBN							
1 ^c	1	H ₂ O, 0.5	CH	P(E/B)-PEO-7, 2	227	0.207	90
2 ^d	1	H ₂ O, 0.5	CH	P(E/B)-PEO-7, 2	216	0.138	85
3 ^e	1	H ₂ O, 0.5	CH	P(E/B)-PEO-7, 2	219	0.135	100
4	1	H ₂ O, 1	CH	Span 60, 15	990 ^f	0.851	90
5	1	H ₂ O, 0.5	CH	P(E/B)-PEO-7, 1.2 Span 60, 15	155	0.242	60 (latex)
6	1	H ₂ O, 1	CH	P(E/B)-PEO-7, 15	333	0.180	100
7	1	H ₂ O, 0.25	CH	P(E/B)-PEO-6, 2	244	0.096	78
8	1	H ₂ O, 0.25	CH	P(E/B)-PEO-7, 2	233	0.171	100
9	1	H ₂ O, 0.25	CH	P(E/B)-PEO-10, 2	263	0.165	80
10	1	H ₂ O, 1	CH	P(E/B)-PEO-7, 2	225	0.082	70
11	0	H ₂ O, 0.5	Isopar M	P(E/B)-PEO-6, 2	179	0.073	60
12	0.05	H ₂ O, 0.5	Isopar M	P(E/B)-PEO-6, 2	291	0.286	100
13	0.1	H ₂ O, 0.5	Isopar M	P(E/B)-PEO-6, 2	279	0.240	100
14	0.25	H ₂ O, 0.5	Isopar M	P(E/B)-PEO-6, 2	320	0.197	100
15	0.5	H ₂ O, 0.5	Isopar M	P(E/B)-PEO-6, 2	261	0.080	83
16	1	H ₂ O, 0.5	Isopar M	P(E/B)-PEO-6, 2	220	0.045	100
17	2	H ₂ O, 0.5	Isopar M	P(E/B)-PEO-6, 2	240	0.065	66
18	1	H ₂ O, 0.5	Isopar M	P(E/B)-PEO-7, 2	217	0.039	100
19	1	H ₂ O, 0.25	Isopar M	P(E/B)-PEO-7, 2	231	0.088	100
20	1	H ₂ O, 0.25	Isopar M	P(E/B)-PEO-6, 2	238	0.071	64
21	1	H ₂ O, 1	Isopar M	P(E/B)-PEO-6, 2	221	0.040	73
22	1	H ₂ O, 1.5	Isopar M	P(E/B)-PEO-6, 2	238	0.050	78
23	1	H ₂ O, 2	Isopar M	P(E/B)-PEO-6, 2	210	0.058	78
24	1	ethanol, 1	CH	P(E/B)-PEO-7, 2	150	0.192	77
25	1	acetone, 1	CH	P(E/B)-PEO-7, 2	152	0.244	51
26	1	AN, 1	CH	P(E/B)-PEO-7, 2	180	0.192	91
27	1	AN, 1	Isopar M	P(E/B)-PEO-7, 2	287	0.122	100
28	1	DMSO, 1	CH	P(E/B)-PEO-7, 2	236	0.139	100
29	1	THF, 1	CH	P(E/B)-PEO-7, 2	149	0.181	40 (latex)
30	1	H ₂ O, 0.25	isooctane	P(E/B)-PEO-6, 2	203	0.151	72
31	1	H ₂ O, 0.25	HD	P(E/B)-PEO-6, 2	229	0.056	100
32	1	H ₂ O, 0.25	HD	P(E/B)-PEO-7 2	203	0.083	60 (latex)
Initiator APS							
33	1	H ₂ O, 0.5	Isopar M	P(E/B)-PEO-7, 2	269	0.121	100
Initiator V59							
34	1	H ₂ O, 0.5	Isopar M	P(E/B)-PEO-7, 2	295	0.231	100

^aHydrodynamic diameter determined by dynamic light scattering (DLS). ^bThe size and width of particle size distribution (as PDI) are calculated from the following equation

$$\ln(G1) = a + b \cdot t + c \cdot t^2 + d \cdot t^3 \quad (1)$$

where $G1$ is a correlation function. The second order cumulant b is converted to a size using the dispersant viscosity and instrumental constants. The coefficient of the squared term c , when scaled as $2c/b^2$ is defined as the polydispersity index (PDI). The PDI is a measure of the particle size distribution and the PDI is a dimensionless number that describes the heterogeneity of the sample; it can range from 0 (monodisperse) to 1 (polydisperse). Values greater than 0.700 indicate a very broad size distribution and a lack of sample homogeneity. ^c2 min of ultrasonication. ^d4 min of ultrasonication. ^e30 min of pulsed sonication (on/off time is 6 s/2 s). ^fMultimodal distribution.

Table 2. Viscosity of Aqueous and Continuous Phase

aqueous phase		continuous phase		
water content (wt %) ^a	viscosity (cP)	nonpolar solvent	viscosity (cP)	
			P(E/B)-PEO-6, 0.5 wt % ^b	P(E/B)-PEO-7, 0.5 wt % ^b
11	~38 ^c	isooctane	0.45 ± 0.02	
20	15.3 ± 3	CH	0.89 ± 0.04	0.91 ± 0.05
33	5.72 ± 0.02	Isopar M	2.12 ± 0.01	2.26 ± 0.01
43	3.64 ± 0.02	HD	3.28 ± 0.02	3.14 ± 0.01
50	2.75 ± 0.03			

^aWith respect to aqueous phase. ^bWith respect to continuous phase. ^cEstimated, see Supporting Information.

scanning calorimeter. Three cycles of heating–cooling were carried out in the temperature range 25–220 °C at 10 °C·min⁻¹. The samples were prepared as for the conversion measurements (see above).

The content of ZnO in the composite latex particles was measured by thermogravimetric analysis (TGA) on a Mettler-Toledo TG/SDTA 851e. About 5 mg of dried sample were heated from 25 to 1100 °C in an oxygen flow.

The heating rate was $10\text{ }^{\circ}\text{C}\cdot\text{min}^{-1}$. Zinc nitrate was converted to ZnO at about $650\text{--}700\text{ }^{\circ}\text{C}$.

A crystallographic study of the white powder received after burning the metal-containing latexes in air at $700\text{ }^{\circ}\text{C}$ was performed on a PANalytical XPert MPD Pro using Cu K α radiation ($\lambda = 0.154\text{ nm}$). The intensity was determined in the range $5^{\circ} < 2\theta < 80^{\circ}$.

The molecular mass of PAAm was estimated by gel-permeation chromatography (GPC) on a Waters chromatograph equipped with a M2410 refractometer and Ultra-hydrogel 2000 and 1000 columns. The flow rate was $1\text{ mL}\cdot\text{min}^{-1}$, and the temperature was kept constant at $30\text{ }^{\circ}\text{C}$. The eluent was prepared by mixing 0.1 M aqueous NaNO_3 and AN in a ratio of 7:3 v:v.²⁰ The salt was added to suppress ion-exclusion effects and AN for the suppression of the inverse-phase retention. Pure PAAm and a mixture of the same PAAm with zinc nitrate showed the same elution volumes in GPC. Thus, the samples could be investigated without dialysis in order to remove the salt. Calibration was performed by narrowly distributed standard PEO samples (Polymer Standards Service-Germany, $M_p = (0.002\text{--}1.7) \times 10^6\text{ g}\cdot\text{mol}^{-1}$). Most of the obtained polymers were not completely soluble in the water/AN mixture and therefore only the soluble part was investigated. Partial insolubility can arise from side reactions like cross-linking and imidization reactions.²¹

For the plasma etching experiments at first the original latex was diluted with CH to 0.5 wt % solid content and a $0.5\text{ }\mu\text{L}$ drop was deposited onto a cleaned silicon substrate. By evaporating the solvent under ambient atmosphere, a hexagonally ordered monolayer of the loaded polymer latexes was obtained. Subsequently, the latexes were exposed to oxygen plasma provided by a commercially available etching device (Plasmalab 80 Plus ICP RIE, Oxford Instruments). For all isotropic etching steps the RIE and the ICP power were 1 and 100 W, respectively. The anisotropic etching was performed with 200 W ICP power while the RIE power was varied between 25 and 50 W.

X-ray photoelectron spectroscopy (XPS) was performed employing nonmonochromatic Al-K α radiation at ambient temperature in an UHV chamber at base pressure of 2×10^{-9} mbar. Photoelectrons were investigated by a SPECS PS-EA10N hemispherical analyzer.

Results and Discussion

Effects of Sonication Time and Type of Sonication. PAAm nanoparticles containing zinc nitrate were prepared by radical polymerization in inverse miniemulsion generated by ultrasonication of the heterophase system. To study the effect of sonication time on particle size and size distribution of the hybrid polymer colloids, besides the composition the sonication power of the ultrasound was kept constant (at 90% amplitude). In addition to continuous sonication of the system, pulsed sonication (on/off time 6 s/2 s) was probed. All syntheses proceeded with quantitative or nearly quantitative yield (Table 1, samples 1, 2, 3, 18). The dependence of the droplet size, polydispersity, and droplet size distribution on the sonication time is shown exemplary for sample 18 (Table 1) in Figure 1. The longer the sonication time is, the narrower is the polydispersity of the droplets. The contribution of fusion and fission processes during emulsification can be evaluated from the number distribution curves (Figure 1a). In the course of sonication the small droplets disappear faster presumably due to fusion than the larger ones due to fission. Turbidity measurements of water emulsions in CH with the polymeric surfactant

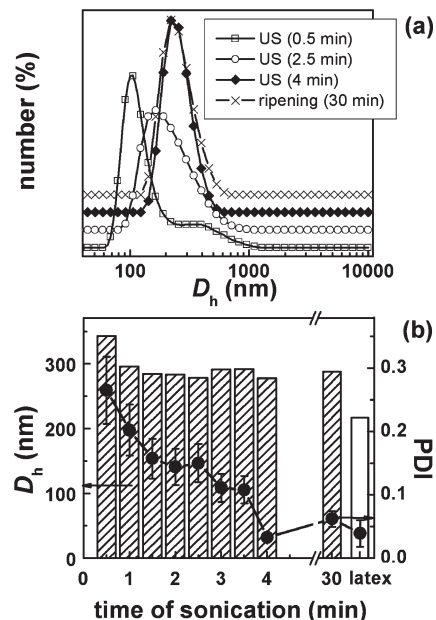


Figure 1. Dependence of (a) droplet size distribution by number and (b) droplet size and polydispersity on the sonication time for sample 18 (see Table 1).

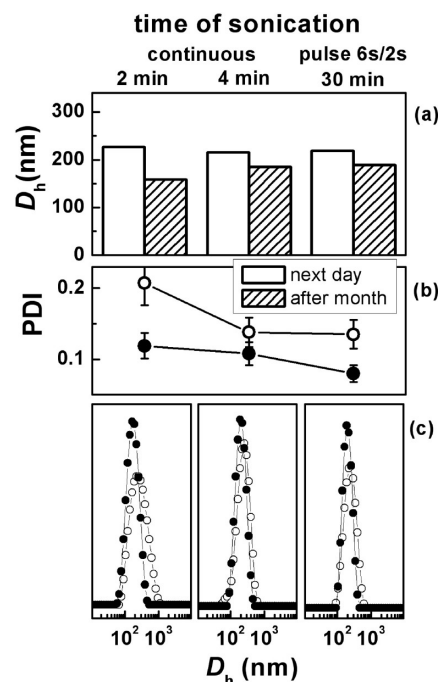


Figure 2. Dependence of (a) size, (b) polydispersity, and (c) particle size distribution on the sonication time for sample 1 (2 min), 2 (4 min), and 3 (pulsed) in Table 1.

poly(ethylene-*co*-butylene)-*b*-poly(ethylene oxide) showed that the steady state of droplet size is reached only after around 1000 s.¹⁵ We determined the polydispersity of sample 18 after 30 min of ripening (Figure 1). The PDI value only slightly increased after this time and the size distribution curves just after sonication (4 min) and after 30 min display an identical shape and position. The common decrease^{18,22} of the particle sizes compared with the initial droplet sizes in miniemulsion arises from the different densities of monomer and polymer, respectively (Figure 1 b). The effect of sonication time on size, polydispersity, and size distribution of the resulting latex particles is shown in Figure 2. It was found

that the polydispersity of the latex particles decreases with an increase in the sonication time up to 4 min, while the average diameter of the particles only marginally decreases, which is in accordance with the behavior of the initial droplet sizes and size distribution. In the case of pulsed treatment, the values of these characteristics were close to the continuous sonication for 4 min. The amount of acoustic energy absorbed by the system during 30 min (6 s/2 s, Table 1, sample 3) of pulsed sonication is equal to one for 22.5 min of continuous sonication. It is known²³ that up to a certain limit, longer sonication times produce finer emulsions, since a larger amount of energy is provided to the medium. Beyond this limit the size of the droplet remains unchanged. Because of the kinetic nature of the size reduction process the geometry of the vessel will affect the energy efficiently absorbed by the system causing the droplet fission. As there is a rapid attenuation of the acoustic waves while moving away from the emitting sonication tip, the hydrodynamics of the vessel can lead to different times at which the final droplet size is achieved, because of the different number of times that a particular element of fluid passes near the sonication tip. Therefore, all miniemulsions were prepared in vessels of the same shape and volume. The stability of the colloids was checked after one month. The polydispersity of the latex with 2 min sonication time was reduced to about the polydispersity of the sample with 4 min sonication time directly after sonication. The decrease of the average diameter after one month was also more pronounced for the first one. This means that 2 min of sonication is insufficient to break the large monomer–salt droplets, which will precipitate as particles after one month. The fraction of these large particles is decreased with increasing the sonication time (increasing total energy dissipation, reducing the non-uniformities).

Effect of Emulsifier. To get insight into the effect of the nature of the emulsifier on the preparation of the initial emulsion the type of emulsifier was varied (Table 1, samples 4, 5, and 6). The latex prepared with 15 wt % of P(E/B)-PEO-7 showed the best monodispersity with a relatively large particle size, whereas the latex prepared with 1.2 wt % of P(E/B)-PEO-7 combined with 15 wt % of Span 60 exhibits a broader distribution, while the latex prepared with only 15 wt % of Span 60 showed the smallest particle size, a multimodal distribution, and the lowest stability with complete phase separation after 1 day. Those results clearly demonstrate that the polymeric surfactant P(E/B)-PEO-7 is an appropriate stabilizer for this emulsification process because of its long chains which provide sufficient steric stabilization even at high amount of salt in the system.

It is known from other systems that the amount of P(E/B)-PEO can be reduced down to 1.5 wt % with respect to the dispersed phase without losing the stability of the latex.¹⁵ In the present work the region of stability of the zinc-containing polymer latexes ranges from 2 wt % to 15 wt % of P(E/B)-PEO-7. Surprisingly, we found contrary to literature reports and our own experience that an increase of the amount of surfactant leads to an increase of the average particle size (Table 1, samples 6 and 10). Although only minor amounts of coagulum (2 wt %) are found, we assume that in the case of the lower concentration of surfactant a significant portion of larger particles forms the coagulum and thus shifts the average diameter and the polydispersity of the stable particles to lower values compared to the case of higher concentration of surfactant. We can not exclude that kinetic effects and/or interactions between the zinc salt and the surfactant have an influence on the particle size and stability of the dispersions.

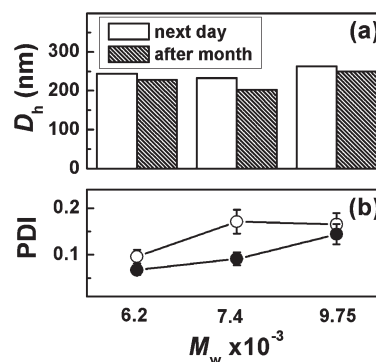


Figure 3. Dependences of (a) size and (b) polydispersity on the molecular mass of P(E/B)-PEO (Table 1, samples 7 (P(E/B)-PEO-6), 8 (P(E/B)-PEO-7), and 9 (P(E/B)-PEO-10)).

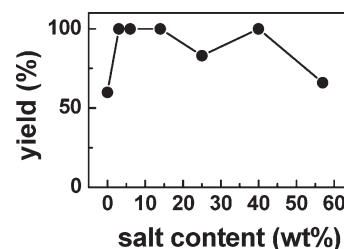


Figure 4. Effect of salt content on the polymer yield.

A similar effect is found for the increase in molecular weight of the hydrophilic block of P(E/B)-PEO (Figure 3, Table 1, samples 7, 8, 9). Only a minor influence of the length of the hydrophilic part of the emulsifier on the particle size is found whereas the polydispersity shows a clear tendency to increase with increasing hydrophilicity of the surfactant which we attribute to the decreasing stability of the dispersions with increasing PEO block. This result is in accordance with the corresponding HLB values. In the case of inverse emulsions nonionic surfactants with HLB values in the range of 4–6 are ideally used (P(E/B)-PEO-6, HLB = 6; see also Supporting Information). Surfactants with HLB values larger than 8 serve rather as wetting agents and emulsifiers for direct emulsions and thus show less good stabilization of inverse emulsions.²⁴

Effect of Zinc Salt Amount. In the next step the effect of the zinc salt on the particle and polymer characteristics was investigated. The study of homogeneous polymerization of AAm in the presence of complexing salts is already described in the literature.²⁵ It was shown that inorganic salts (such as LiBr, LiCl, CaCl₂) in solvents having a relatively low polarity and no basic properties greatly affect the kinetic parameters of the polymerization process and the molecular characteristics of the resulting PAAM. This effect was assigned to the formation of a complex of the metal ions with the monomer and also with the growing polymeric radicals changing the reactivity of the reacting species. It was also shown that in the case of ZnCl₂ the rate of polymerization greatly increases only when water was added to the reaction medium (THF) as only in water ZnCl₂ is present in the ionized state. In our work the amount of salt in the system was changed from 0 wt % up to 57 wt % (Table 1, samples 11–17). Relatively lower polymer yield was observed at the limit values of this region (Figure 4). Within the region polymer was formed in (almost) quantitative yield. The molecular masses determined by GPC lay above the calibration range of the PEO standards (up to 1.7×10^6 g mol⁻¹) indicating the formation of high molecular weight polymers. We assume that the salt, besides

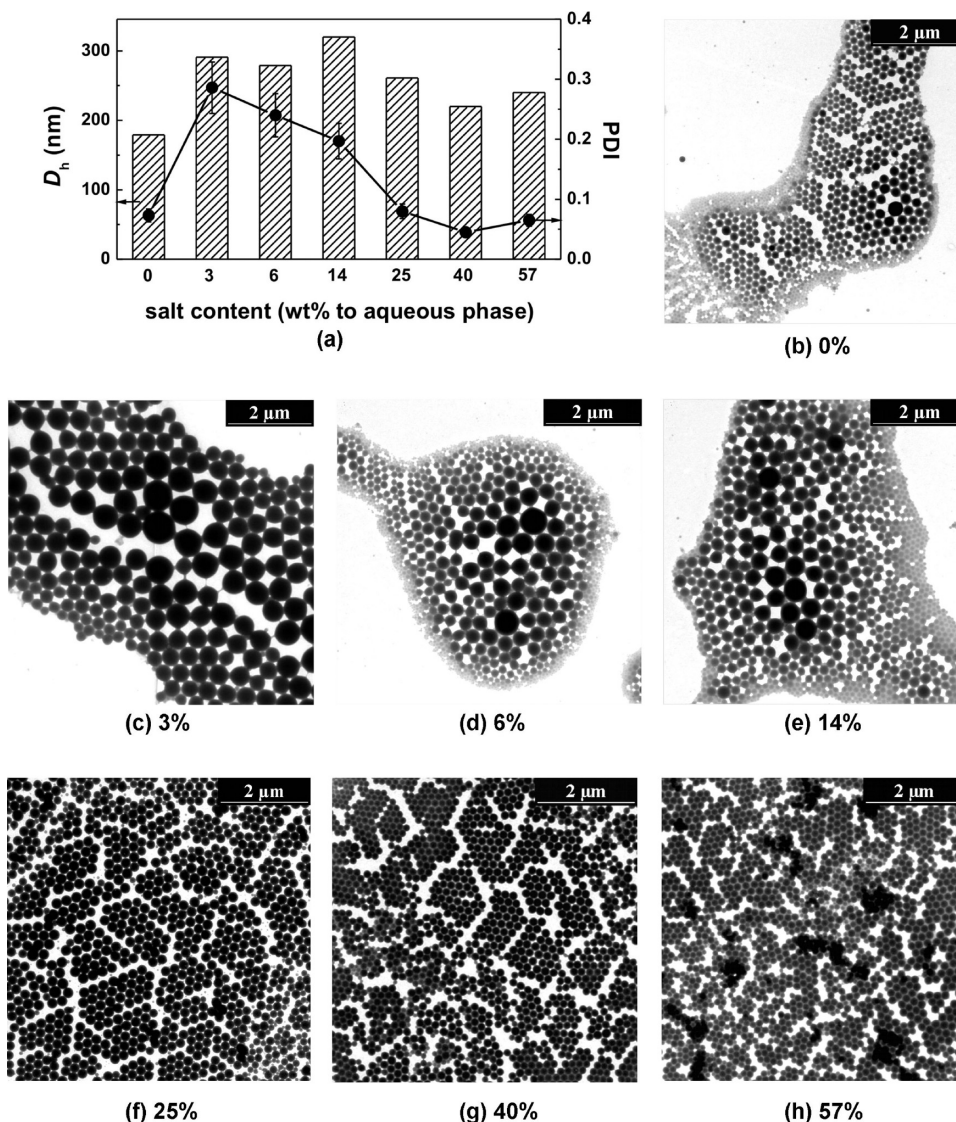


Figure 5. (a) Dependence of the particle size and polydispersity for zinc-containing polymer latexes on different amounts of salt (see Table 1: sample 11, 0 wt %; sample 12, 3 wt %; sample 13, 6 wt %; sample 14, 14 wt %; sample 15, 25 wt %; sample 16, 40 wt %; sample 17, 57 wt %); (b–h) TEM micrographs of latexes prepared with different salt amounts.

its function as Ostwald ripening agent, forms complexes with growing macroradicals resulting in an increased molecular weight, similar to the polymerization of AAm in water.^{21,25} Partial insolubility of PAAM can arise from side reactions like cross-linking and branching at high initiator concentrations,²¹ imidization reactions forced by temperature (above 60 °C)²¹ and a low pH of the dispersed medium ($\sim 3-4$).^{26,27} The sample with the best solubility in water was sample 16 at 40 wt % of zinc salt. The molar ratio of AAm and Zn-(NO₃)₂·6H₂O in this synthesis was 4:1 in agreement with the stoichiometry of the suggested structure of a complex Zn-(NO₃)₂AAM₄·2H₂O as already described in the literature.²⁸ In addition, we observed that an increase of the amount of salt enhanced the solubility of AAm in the aqueous phase which also points to the formation of the complex. This finding further supports our assumption that the complexation has a significant effect on the molecular characteristics of the resulting polymer.

The glass transition temperatures (T_g) of the composite nanoparticles were measured by DSC (see Supporting Information). Depending on the amount of salt in the particles, the T_g decreased from 195 °C for pure PAAM particles down to

179 °C for latex containing 14 wt % of salt presumably due to a plasticizing effect of the salt. The decomposition temperature T_d of the polymers also decreased with increasing salt content but more rapidly than the glass transition temperature T_g . For example, for the sample containing 25 wt % of salt T_d lies at about 150 °C. Therefore, samples with higher contents of salt could not be determined by DSC as it resulted in destruction of the polymer before T_g was reached. Apparently there is a strong interaction between the polymeric matrix and the salt.

The dependence of particle size and polydispersity for the zinc-containing polymer latexes on different amounts of salt are shown in Figure 5a. Despite of the low PDI value for PAAM latex without salt determined by DLS visually a higher polydispersity is found in TEM images (Figure 5a, b). More monodisperse samples were observed with salt contents above 25 wt % (Figure 5f–h). It is mentioned in the literature that the addition of salt and AAm to the aqueous phase of a miniemulsion decreases the interfacial tension²² which we assume to be the reason for the narrowing particle size distribution with increasing salt content.

Effect of Initiator. The influence of the nucleation mechanism on the particle size and size distribution was studied by

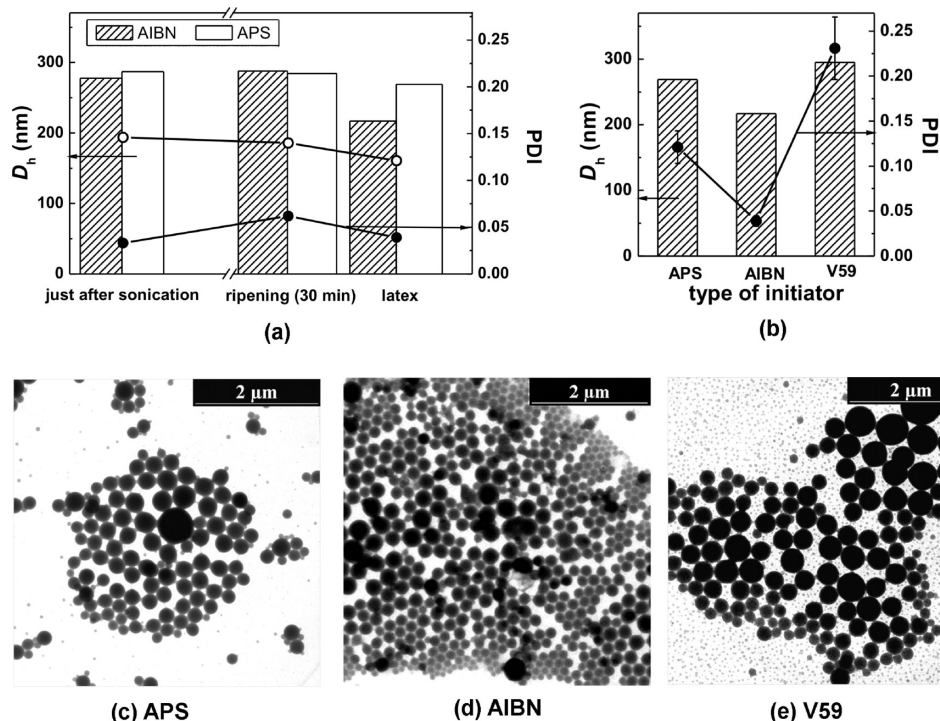


Figure 6. (a) Dependence of the droplet and particle size and polydispersity on the type of initiator; (b) dependence of the particle size and polydispersity on the type of initiator; (c) TEM micrograph of latex prepared under APS initiation (see Table 1, sample 33); (d) TEM micrograph of latex prepared under AIBN initiation (see Table 1, sample 18); (e) TEM micrograph of latex prepared under V59 initiation (see Table 1, sample 34).

changing the nature of the initiator and the dispersed medium, respectively (see section below, Effect of Polar Solvents in the Dispersed Phase). It was expected that in the case of the water-soluble initiator, APS, the droplet nucleation would predominate and the narrowest polydispersity should be observed. For hydrophobic initiators (AIBN and V59), a broadening of the particle size distribution might be observed because of secondary nucleation. Contrary, the best monodispersity was observed for the system with AIBN initiation (Figure 6a,b). The reason for high polydispersity in the case of APS initiation is rather attributed to the emulsion preparation procedure. Because of the high concentration of AAm in solution the initiation with APS started already during the miniemulsification process promoted by the increase of the system temperature due to ultrasonication despite of ice cooling. Thus, the droplet size distribution in the case of the just prepared miniemulsion was narrower for AIBN than for APS as initiator (Figure 6a). Moreover, the PDI value for the miniemulsion with APS was close to the PDI value for the system with AIBN after 2 min of sonication and did not change greatly during the synthesis (Figure 1b and Figure 6a). Therefore, we assume that in our case the system did not reach the equilibrium and the size distribution of the latex particles reflects the droplet size distribution of the less stabilized emulsion (Figure 6c). In addition, there might be a detrimental interaction between the ionic initiator and the zinc salt. The oil-soluble nonionic initiators were added to the emulsion 30 min after miniemulsification to avoid premature polymerization (see above). In the system with the most hydrophobic initiator V59 TEM analysis reveals two populations of latex particles (Figure 6e). Smaller particles ($D \sim 30$ nm) are polymer particles generated by secondary nucleation. Larger particles were created by droplet nucleation. Finally, from the TEM micrograph of latex particles initiated by AIBN in Figure 6d, a lower polydispersity and mainly latex particles produced by droplet nucleation are observed. This might be caused by

the higher solubility of AIBN in water than V59 which is even more pronounced in the presence of a large amount of AAm and thus droplet nucleation is more favored.²⁹

Effect of Solvent Amount. The influence of solvent content in the dispersed phase on the particle size and size distribution of zinc-containing polymer latexes was studied by varying the amount of water at a salt content of 40 wt % and a molar ratio of AAm and salt of 4:1. AIBN was used as initiator. As water will have a plasticizing effect on the resulting latexes the content should be kept at a minimum in order to avoid complications during the etching process (see below). The lowest water content still forming a homogeneous phase with the monomer and the zinc salt was 11 wt % at ca. 45 °C compared to a saturated solution of pure AAm with about 40 wt % water at 20 °C.³⁰ The optimal water content was found at 20 wt % for the preparation of water-soluble polymers with high yield. The effect of solvent content in the dispersed phase on the particle size and size distribution of zinc-containing polymer latexes is shown in Figure 7. No big changes in average particle size (~ 225 nm) were found for water contents ranging between 11 and 50 wt %. Usually, in miniemulsion polymerization the droplet size and subsequently the size of the latex particles can be modified by varying the amount of emulsifier.¹⁵ In this case the ratio of emulsifier/aqueous phase was kept constant. The change of the nature of the oil phase also had no effect on the particle size (see section below: Effect of Viscosity of the Continuous Phase). However, the dilution of the AAm phase positively affected the monodispersity of the system (Figure 7 and Figure 8). Thus, in the case of Isopar M as continuous phase the polydispersity decreased from 0.071 down to 0.040–0.060 and even more pronounced for CH from 0.171 to 0.082). The main role in this reduction probably plays the viscosity of the dispersed phase as a measure of molecular interactions in the liquid. The viscosity is drastically increased with a decrease of water content (Table 2). The higher the viscosity, the higher the attractive forces between

the molecules and, therefore, it is more difficult to overcome cohesive forces of the liquid at higher viscosities.

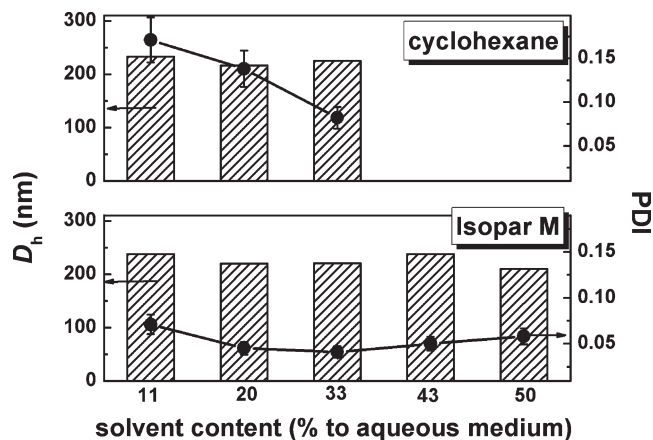


Figure 7. Dependence of the particle size and polydispersity for zinc-containing polymer latexes on different amount of solvent with (a) CH as continuous phase (see Tab. 1: sample 8, 11 wt %; sample 2, 20 wt %; sample 10, 33 wt %), and (b) Isopar M as continuous phase (see Table 1: sample 20, 11 wt %; sample 16, 20 wt %; sample 21, 33 wt %; sample 22, 43 wt %).

Effect of the Nature of the Polar Solvents in the Dispersed Phase. The mechanism of particle formation and the type of nucleation can be changed not only by varying the nature of the initiator (see section above, Effect of Initiator) but also by changing the nature of the dispersed medium. Thus, a miniemulsion polymerization process can be complicated by dispersion polymerization if solvents for AAm are used which are miscible with CH like ethanol, acetone, or THF. Here, the continuous phase comprises solvents for the monomers but not for the resulting polymer. The polymer is formed in the continuous phase and precipitates as small particles when the growing polymer chains exceed a critical chain length. Then, these initial particles aggregate and form stable particles stabilized by surfactants. At the same time in the system proceeded droplet nucleation since the polar phase was only partially miscible with CH and the initial system consisted of two phases. So, the growing chains can lead to secondary nucleation as well as diffuse to monomer-swollen polymer particles. As it is expected from this agglomeration mechanism the polydispersities of such colloids are very high (Figure 9 (phase I), Figure 10a). The yield of polymer in this case is lowest because of additional side reactions, for example chain transfer to the solvent (Table 1, samples 24, 25, 29).³¹

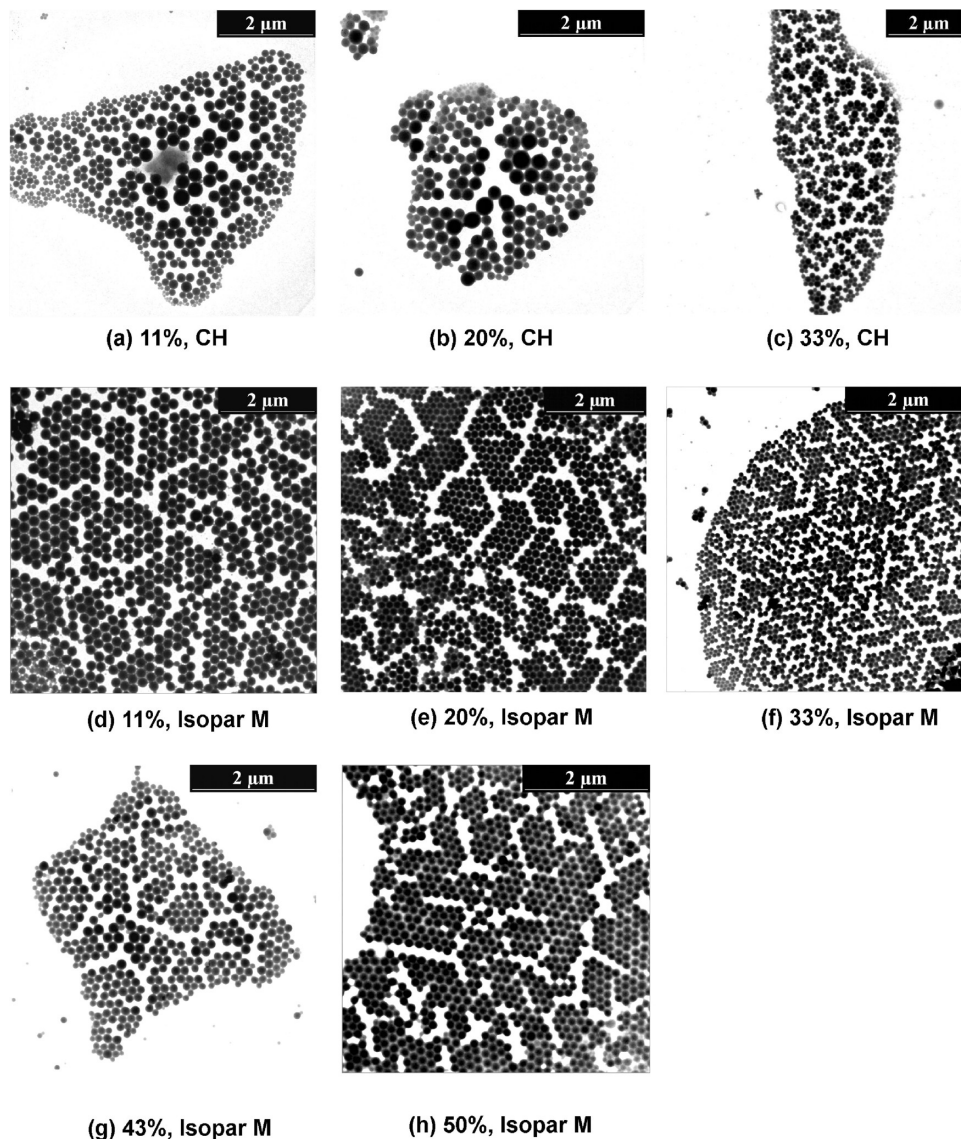


Figure 8. TEM micrograph of latex prepared with different amounts of solvent (see Table 1 and Figure 7).

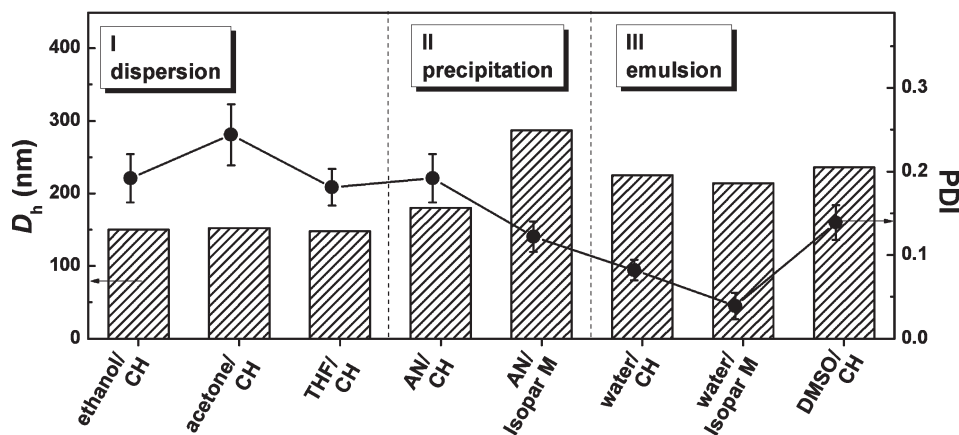


Figure 9. Dependence of the particle size and polydispersity for zinc-containing polymer latexes on the nature of dispersed and continuous phases (see Table 1).

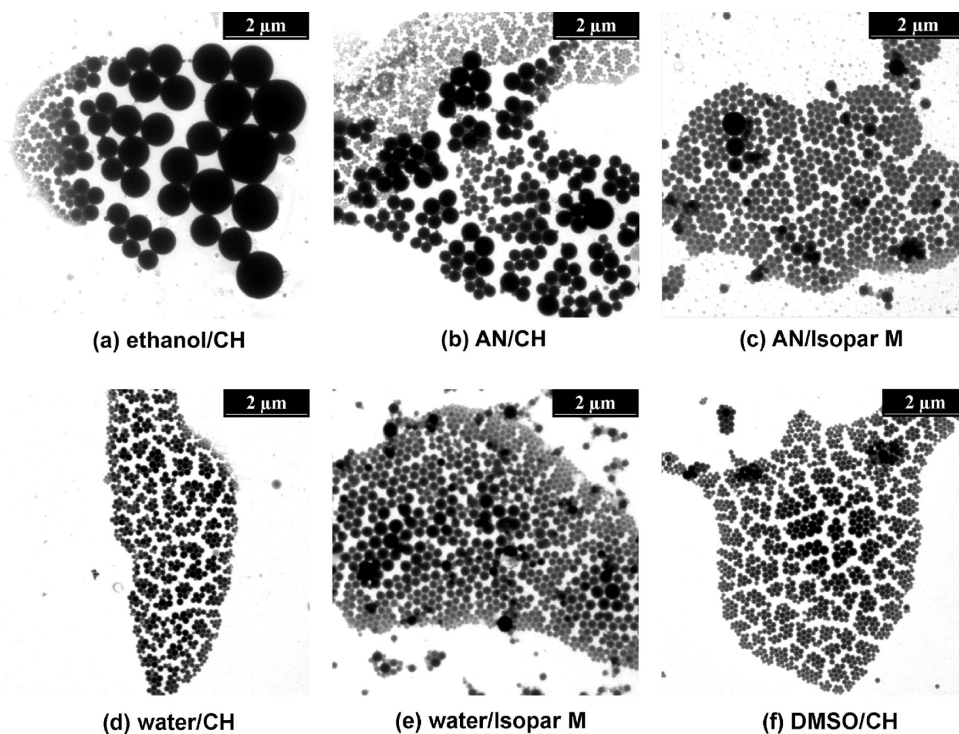


Figure 10. TEM micrograph of latex prepared in different systems (see Table 1 and Figure 9).

In the case of AN a combination of emulsion and precipitation polymerization takes place (Table 1, samples 26, 27). The initial solution of monomer and salt in AN forms an emulsion in oil but the polymerization in each droplet is precipitation by its nature. The polymers were obtained with quantitative yield. Polymerization with CH as continuous medium resulted in water-soluble products with high molecular mass. The use of Isopar M gave a partially water-soluble polymer. Probably the elimination of heat in this system is more difficult due to the more viscous continuous medium, and partially cross-linking and imidization reactions take place. On the other side a more monodisperse sample was observed in the case of Isopar M (Figure 9II, Figure 10c).

The emulsion polymerization proceeded when solvents for AAm as well as for PAAm were used. High polymer yield and partial water solubility of the polymer characterize these systems (Table 1, samples 10, 18, 28). The latex particle size was about 226 nm independent of the solvent type. The lowest polydispersity was observed for this type of

polymerization compared to the mechanisms discussed above (Figure 9III, Figure 10d–f). Similar to the case of AN, the more monodisperse sample was observed in the case of Isopar M as continuous phase.

Effect of Viscosity of the Continuous Phase. The influence of the viscosity of the continuous medium on the particle size and size distribution of zinc-containing polymer latexes has been studied by varying the nature of the oil (Table 1, samples 7, 8, 19, 20, 30, 31, and 32, and Table 2). As can be seen in Figure 11 no big changes in the average droplet size (about 225 nm) are found for oil viscosities ranging between 0.453 and 3.28 cP. These results are in accordance with size dependences observed for W/O systems with varying the viscosity values from 2.6 up to 1850 cP.³² This behavior is attributed to the independence of the intensity of the bubble collapse on the liquid viscosity when the onset of cavitation is reached.³² Moreover, because of the heterogeneous system, cavitation will preferably occur at the interface or even in the aqueous droplets. However, we found that the viscosity of

the continuous phase had a great influence on the polydispersity of the latex particles. The higher the viscosity of the medium the more homogeneous particles were observed (Figure 11 and Figure 12). The same trend was found in the case of miniemulsion polymerization of 2-hydroxyethyl methacrylate.³³ Here the authors demonstrated that an improved droplet stability causes a narrower size distribution which can be controlled by adjusting the interfacial tension, osmotic pressure, and viscosity of the system. It was shown that the interfacial tensions between polar and non-polar phases decreased in the order of HD > isopar M > isooctane > CH. The lower the interfacial tension is, the more easily the liquid can be disrupted and more monodisperse

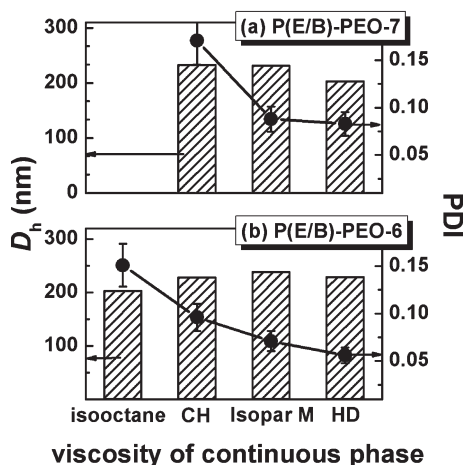


Figure 11. Dependence of the particle size and polydispersity for zinc-containing polymer latexes on the viscosity of the continuous phase with (a) P(E/B)-PEO-7 as emulsifier (see Table 1: sample 8, CH; sample 19, Isopar M; sample 32, HD) and (b) P(E/B)-PEO-6 as emulsifier (see Table 1: sample 30, sample isooctane; 7, CH; sample 20, Isopar M; sample 31, HD).

systems are observed in the case of low viscous continuous phases, i.e., isooctane and CH. In the case of more hydrophobic and viscous Isopar M and HD the dependence of the interfacial tension and monodispersity shows the opposite tendency. The same unexpected observation was made in the case of water/paraffin (light) oil (viscosity = 24.58 cP, interfacial tension = 40.9 mN/m) and water/paraffin (heavy) oil (viscosity = 54.65 cP, interfacial tension = 67 mN/m) inverse emulsions at irradiation times of 10 min.²³ This was attributed to the high viscosity of the paraffin (heavy) oil. Since the settling velocity of droplets is inverse to the viscosity, the higher the viscosity the lower is the coalescence of droplets resulting in improved droplet stability and decreased polydispersity.

TGA Measurements. The amount of solid residual in TGA measurement was within the experimental accuracy in agreement with the theoretical value for ZnO in the sample. The crystallographic study of the solid confirmed the presence of polycrystalline hexagonal wurtzite type ZnO.³⁴

Plasma Etching. To show the applicability of the synthesized composite particles for the preparation of ZnO nanoparticles arrays a plasma etching process similar to corresponding experiments with metal-precursor-containing polystyrene colloids was performed.^{13,14} Since in the case of polystyrene the plasma etching process was adjusted for small amounts of salt, in the present investigation a sample with low content of salt was also chosen (Table 1, sample 13). Despite of the high polydispersity of the sample some areas of highly ordered initial composite particles with a narrow size distribution could be found. After the application of isotropic oxygen plasma for 10 min these areas were converted into highly ordered arrays of particles containing ZnO nanocrystals. As example the area of particles with an average diameter of ca. 14 nm and interparticle distances of ca. 66 nm are shown in Figure 13. The interparticle distance originates from the initial diameter of PAAm particles, while the hexagonal order is a result of the self-assembly

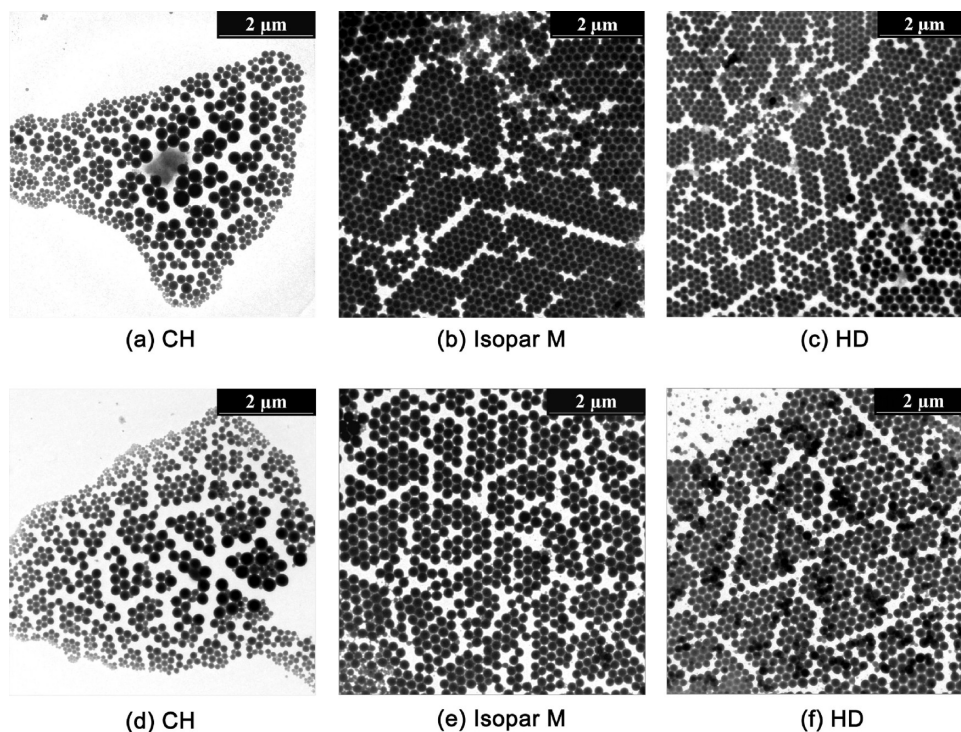


Figure 12. TEM micrograph of latex prepared with P(E/B)-PEO-7 (a–c) and P(E/B)-PEO-6 (d–f) in different continuous media (see Table 1 and Figure 11).

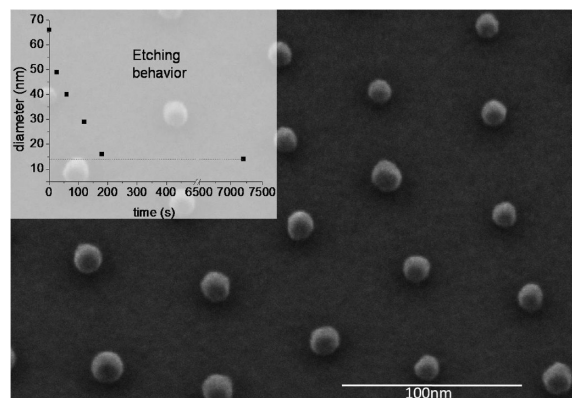


Figure 13. Monolayer of PAAm hybrid particles deposited onto a silicon substrate and exposed to a plasma etching process (SEM, tilted 30°). The average initial particle diameter of 66 nm approaches its final “saturated” value of 14 nm in diameter as shown in the inset.

on the Si substrate. The expected diameter of the ZnO particles calculated from the loading of the PAAm particles with zinc salt is ca. 11 nm and hence distinctly smaller than the measured diameter.

HRSEM investigations show that the plasma treatment shrinks the loaded PAAm particles toward a saturated state (Figure 13). A saturated state was reported recently for platinum precursor loaded PS particles after oxygen plasma exposure.¹³ HRTEM measurements of the etched PAAm hybrid particles prove that the particles of this saturated state consist of a spherical agglomeration of tiny single crystalline ZnO particles with diameters of 1–2 nm in a still unknown matrix. The volume of this agglomeration is about 1.8 times larger than the expected volume calculated from the net weight of Zn precursor, assuming stoichiometric ZnO in the hexagonal wurtzite structure.

Additional X-ray photoelectron spectroscopy investigations (not shown) of the final etching state confirm the dissociation of the Zn precursor, the generation of ZnO, the absence of metallic Zn, and the loss of N from the precursor.

Following the processing in ref 13, further annealing steps should lead to pure ZnO particles. This approach is currently under investigation.

Conclusion

In the present work composite nanoparticles based on PAAm and zinc nitrate were successfully prepared by inverse miniemulsion polymerization. Various factors influenced the polydispersity of the resulting hybrid particles. Thus, the miniemulsion technique was found to be the best for the preparation of zinc-containing latexes with quantitative yield and low polydispersity of the latex particles compared to dispersion, precipitation or a combination of several polymerization types. The investigation of the parameters affecting the preparation of the initial emulsion showed that 4 min of ultrasonication and using an amphiphilic polymeric surfactant with a relatively short hydrophilic part improved both the monodispersity and the stability of the latexes. An increase in viscosity of the continuous phase (changed by the addition of different nonpolar solvents) and dilution of the dispersed phase by water also reduced the polydispersity of the latex particles. The use of AIBN as initiator which partially redistributed between the emulsion phases reduced the fraction of small pure polymer particles generated by secondary nucleation.

It was found that complexation between AAm and zinc nitrate affected the solubility as well as the yield of the polymers. Both were increased when the molar ratio of AAm and

Zn(NO₃)₂·6H₂O was chosen 4:1 corresponding to the complex Zn(NO₃)₂·AAm₄·2H₂O already reported in the literature.²⁸ The monodispersity of the latex particles was also improved when the salt:monomer ratio was close to this value.

Some preliminary results concerning applicability of these composite particles were shown. Thus, the samples with a low content of salt were subjected to a plasma etching process. Highly ordered arrays of particles containing ZnO nanocrystals were observed. Future effort will be devoted to an improvement of the process regarding polymer and colloidal characteristics like ideal initiator and surfactant and an optimization of the plasma etching procedure.

Acknowledgment. The authors thank G. Weber for providing us with polymeric surfactants, P(E/B)-PEO, and for the TGA measurements, Dr. C. Hoffmann-Richter for the DSC measurements, M. Wendel for the GPC measurements (all Institute of Organic Chemistry III, University of Ulm), and S. Blessing (Institute of Inorganic Chemistry I, University of Ulm) for the XRD measurements. The support by Deutsche Forschungsgemeinschaft (DFG) within the Cooperative Research Center SFB 569 is gratefully acknowledged.

Supporting Information Available: Text giving a detailed procedure for the characterization of P(E/B)–PEO and figures showing a supporting graph for the calculation of the viscosity of the aqueous phase and the dependence of T_g on the salt content. This material is available free of charge via the Internet at <http://pubs.acs.org>.

References and Notes

- Yuan, F.; Peng, H.; Yin, Y.; Chunlei, Y.; Ryu, H. *Mater. Sci. Eng., B* **2005**, *122*, 55–60.
- Singla, M. L.; Shafeeq, M. M.; Kumar, M. *J. Lumin.* **2009**, *129*, 434–438.
- Li, X.; He, G.; Xiao, G.; Liu, H.; Wang, M. *J. Colloid Interface Sci.* **2009**, *333*, 465–473.
- Hong, R. Y.; Li, J. H.; Chen, L. L.; Liu, D. Q.; Li, H. Z.; Zheng, Y.; Ding, J. *Powder Technol.* **2009**, *189*, 426–432.
- Demir, M. M.; Memesa, M.; Castignolles, P.; Wegner, G. *Macromol. Rapid Commun.* **2006**, *27*, 763–770.
- Luo, Y.-D.; Dai, C.-A.; Chiu, W.-Y. *J. Polym. Sci., Part A: Polym. Chem.* **2008**, *46*, 8081–8090.
- Choy, J.-H.; Jang, E. S.; Won, J. H.; Chung, J. H.; Jang, D. J.; Kim, Y. W. *Adv. Mater.* **2003**, *15*, 1911–1914.
- Spatz, J. P.; Mossmer, S.; Hartmann, C.; Moller, M.; Herzog, T.; Krieger, M.; Boyen, H.-G.; Ziemann, P.; Kabius, B. *Langmuir* **2000**, *16*, 407–415.
- Landfester, K. *Annu. Rev. Mater. Res.* **2006**, *36*, 231–279.
- Luo, Y.-D.; Dai, C.-A.; Chiu, W.-Y. *J. Polym. Sci., Part A: Polym. Chem.* **2008**, *46*, 1014–1024.
- Ramirez, L. P.; Landfester, K. *Macromol. Chem. Phys.* **2003**, *204*, 22–31.
- Xu, Z. Z.; Wang, C. C.; Yang, W. L.; Deng, Y. H.; Fu, S. K. *J. Magn. Magn. Mater.* **2004**, *277*, 136–143.
- Manzke, A.; Pfahler, C.; Dubbers, O.; Plettl, A.; Ziemann, P.; Crespy, D.; Schreiber, E.; Ziener, U.; Landfester, K. *Adv. Mater.* **2007**, *19*, 1337–1341.
- Schreiber, E.; Ziener, U.; Manzke, A.; Plettl, A.; Ziemann, P.; Landfester, K. *Chem. Mater.* **2009**, *21*, 1750–1760.
- Landfester, K.; Willert, M.; Antonietti, M. *Macromolecules* **2000**, *33*, 2370–2376.
- Oh, J. K.; Dong, H.; Zhang, R.; Matyjaszewski, K.; Schlaad, H. *J. Polym. Sci., Part A: Polym. Chem.* **2007**, *45*, 4764–4772.
- Gengeng, Q.; Christopher, W. J.; Schork, F. J. *Macromol. Rapid Commun.* **2007**, *28*, 1010–1016.
- Blagodatskikh, I.; Tikhonov, V.; Ivanova, E.; Landfester, K.; Khokhlov, A. *Macromol. Rapid Commun.* **2006**, *27*, 1900–1905.
- Thomas, A.; Schlaad, H.; Smarsly, B.; Antonietti, M. *Langmuir* **2003**, *19*, 4455–4459.
- Blagodatskikh, I. V.; Vasil'eva, O. V.; Ivanova, E. M.; Bykov, S. V.; Churochkina, N. A.; Pryakhina, T. A.; Smirnov, V. A.; Philippova, O. E.; Khokhlov, A. R. *Polymer* **2004**, *45*, 5897–5904.

- (21) Kurenkov, V. F.; Myagchenkov, V. A. *Polym. Plast. Technol. Eng.* **1991**, *30*, 367–404.
- (22) Ivanova, E.; Blagodatskikh, I.; Vasil'eva, O.; Barabanova, A.; Khokhlov, A. *Polym. Sci., A* **2008**, *50*, 9–17.
- (23) Gaikwad, S. G.; Pandit, A. B. *Ultrason. Sonochem.* **2008**, *15*, 554–563.
- (24) Adamson, A. W.; Gast, A. P. *Physical chemistry of surfaces*, 6th ed.; Wiley: New York, 1997; p 784.
- (25) Gromov, V. F. *Russ. Chem. Rev.* **1995**, *64*, 87–97.
- (26) Dainton, F. S.; Tordoff, M. *Trans. Faraday Soc.* **1957**, *53*, 499–511.
- (27) Currie, D. J.; Dainton, F. S.; Watt, W. S. *Polymer* **1965**, *6*, 451–453.
- (28) Dzhardimalieva, G. I.; Pomogailo, A. D.; Volpert, V. A. *J. Inorg. Organomet. Polym.* **2002**, *12*, 1–21.
- (29) Gromov, V. F.; Osmanov, T. O.; Glazkova, I. V.; Gritiskova, I. A.; Teleshov, E. N. *Polym. Sci. USSR* **1988**, *30*, 1210–1215.
- (30) Gromov, V. F.; Sheinker, A. P.; Khomikovskii, P. M.; Abkin, A. D. *Polym. Sci. USSR* **1974**, *16*, 423–429.
- (31) Vascaronková, V.; Oremusová, D.; Barton, J. *Makromol. Chem.* **1988**, *189*, 709–713.
- (32) Behrend, O.; Ax, K.; Schubert, H. *Ultrason. Sonochem.* **2000**, *7*, 77–85.
- (33) Cao, Z.; Wang, Z.; Herrmann, C.; Ziener, U.; Landfester, K. *Langmuir* **2010**, in press. DOI: 10.1021/la904380k.
- (34) Ning, G.-H.; Zhao, X.-P.; Li, J.; Zhang, C.-Q. *Opt. Mater.* **2006**, *28*, 385–390.